# Effects of dynamic axial stiffness of elastic moorings for a wave energy converter



Citation for the original published paper (version of record):
Depalo, F., Wang, S., Xu, S. et al (2022). Effects of dynamic axial stiffness of elastic moorings for a wave energy converter. Ocean Engineering, 251. http://dx.doi.org/10.1016/j.oceaneng.2022.111132

Ocean Engineering 251 (2022) 111132

Contents lists available at ScienceDirect

Ocean Engineering

journal homepage: www.elsevier.com/locate/oceaneng

# Effects of dynamic axial stiffness of elastic moorings for a wave energy converter

Francesco Depalo [a], Shan Wang [a], Sheng Xu [a], C. Guedes Soares [a,*], Shun-Han Yang [b], Jonas W. Ringsberg [b]

[a] Centre for Marine Technology and Ocean Engineering (CENTEC), Instituto Superior Técnico, Universidade de Lisboa, Av. Rovisco Pais, 1049-001, Lisboa, Portugal
[b] Chalmers University of Technology, Department of Mechanics and Maritime Sciences, Division of Marine Technology, SE-412 96, Gothenburg, Sweden

ARTICLE INFO

*Keywords:*
Dynamic axial stiffness
Elastic cables
Wave energy converter
DeepC

ABSTRACT

This work studies the effects of the dynamic axial stiffness of elastic moorings on the dynamic behaviour of a point absorber wave energy converter. Following two mooring analysis procedures, coupled dynamic analysis of a taut-moored WEC with three legs is performed using the FEM program DeepC in three irregular wave conditions. Two synthetic fibre rope materials are investigated, i.e. a normally stiff polyester and a wire-lay 3-strand nylon rope. The results of WEC motions and mooring tensions obtained from a quasi-static stiffness model and the dynamic stiffness model are compared and discussed. The former analysis applies the non-linear stiffness working curves of the ropes in the simulations, while the latter utilizes the dynamic stiffness expression with an iterative process following a practical mooring analysis procedure. For the nylon rope, the influence of the load amplitude on the dynamic stiffness and the WEC response is presented and analysed. It was found that the quasi-static stiffness model tends to underestimate the maximum mooring tensions, leading to 30%–40% lower results compared to the one accounting for the dynamic stiffness effects. For the studied WEC system, the nylon rope shows advantages over polyester, because of the lower mooring tensions and higher WEC motions.

## 1. Introduction

Wave energy converters are considered one of the most promising clean energy sources in the world of renewable energy. These devices convert the kinetic and potential energy of a sea wave into useful mechanical or electrical energy. The potential of this energy source is extremely wide, but this type of system is relatively recent and most of them are still in the preliminary study phase (Cruz, 2007; Czech and Bauer, 2012). Compared to nearshore regions, offshore locations present significantly larger amounts of wave energy and free sea space, which could facilitate the deployment of larger numbers of wave energy converters (WECs).

For conventional floating structures, mooring is an important component to assure survivability during extreme sea states. For floating WECs, the mooring system is important, not only for station keeping but also it can be a part of the power take-off (PTO) mechanism and may have a direct influence on the energy extraction efficiency of the device. The cost of the mooring system for WECs takes 10%–30% (Martinelli et al., 2012; Thomsen, 2015) of the overall capital costs in contrast to only 2% for oil and gas offshore platforms (Fitzgerald, 2009). In view of this, Thomsen et al. (2018) carried out an optimization study on the costs of mooring solutions for four large WECs, finding that the line diameter provided the largest impact on the mooring cost. The mooring design is also relevant to the working principle of WECs. For the motion-independent devices (e.g., OWC), the mooring design is similar to conventional oil and gas platforms, i.e., the resonant period of mooring should be designed outside the wave period to reduce dynamic loads. On the contrary, for the motion-dependent device, the mooring system needs to be designed to make the resonant period of energy extraction primary modes match the classical wave period of the target site as close as possible (Cribbs et al., 2017).

Extensive experiences on mooring designs in the offshore oil and gas industry have provided useful references to mooring system design of WECs (Guedes Soares et al., 2012), however, Weller et al. (2013) also mentioned that applying existing offshore design guidelines or codes to the wave energy devices is not a straightforward process and can lead to conservative designs. Johanning et al. (2005) discussed in detail how the existing mooring standards from the oil and gas industry fitted in the

* Corresponding author.
*E-mail address:* c.guedes.soares@centec.tecnico.ulisboa.pt (C. Guedes Soares).

https://doi.org/10.1016/j.oceaneng.2022.111132
Received 8 October 2021; Received in revised form 16 February 2022; Accepted 17 March 2022
Available online 7 April 2022

application of station-keeping of WECs. The main differences between WECs mooring systems compared to those from other offshore applications were discussed in Cribbs et al. (2017), including water depth, designed natural frequencies, structure scale, allow-able motion amplitudes, mooring system footprint and the number of mooring lines, accounting for PTO characteristics, a lower return period and relatively high cost. Despite this, there are still some useful references on general offshore structures. For example, Chakrabarti (2005) published a book that covers the basic background materials and their application in offshore engineering, with the emphasis on the application of the theory to practical problems. It includes the practical aspects of the offshore structures with handy design guides. Ma et al. (2019) introduced in-depth knowledge on all aspects of mooring systems, from design and analysis to installation, operation, maintenance, and integrity management for offshore structures. In addition, a static method for preliminary mooring design for WECs was introduced to determine the initial mooring configuration, line properties and mooring pretension with the estimated mean environmental loads.

As the research on mooring design for WECs is becoming more and more attractive, some mooring design procedures for WECs can be found in the literature, such as Johanning et al. (2006a, 2006b). Martinelli et al. (2012), Bergdahl and Kofoed (2015), Thomsen et al. (2017, 2018), Weller et al. (2018), Xu et al. (2019), Doyle et al. (2019), Giannini et al. (2020), Depalo et al. (2021). Among these, the importance of the pre-tension and choice of both mooring material and geometry in determining the stiffness characteristics of a mooring system for a floating WEC was studied by Johanning et al. (2006a, 2006b). They concluded that a good understanding of the related stiffness and motion characteristics is essential to develop suitable design guidance that would address not only the issue of line failure but also satisfy the requirement for high-energy conversion efficiency.

A preliminary design of a floating offshore version of CECO was presented in Giannini et al. (2020) which concluded that particular attention should be paid to mooring system design, in terms of properties and materials selection, to increase efficiency and at the same time reduce extreme mooring loads and fatigue. Mooring and foundation design of marine renewable energy (MRE) devices was performed in Weller et al. (2018) using an open-source solution DTOcean (Optimal Design Tools for Ocean Energy Arrays), which can capture several key aspects of MRE array design and provide the design with lowest capital cost. Besides, there is a wide range of design guidelines, such as DNV (2018), API-RP-2SK (2005), and ISO, 2013.

In addition to the preliminary design, numerical analysis is an essential step in predicting the dynamic responses of WEC systems. An extensive review of mathematic modelling of mooring systems for WECs was made by Davidson and Ringwood (2017), while the performance of different commercial analysis tools in the application of WEC mooring design is assessed in Thomsen et al. (2017a,b) which highlighted the two packages DeepC (DNV, 2004; DNV, 2013a, 3013b) and OrcaFlex as potential software solutions in mooring analysis. The effects of the wave-induced response of floating CALM buoys on the load combination of submarine hose systems and sensitivity studies were performed by the Amaechi et al. (2019) using the hydrodynamic models developed using ANSYS AQWA and the coupled simulation in Orcaflex. Yang et al. (2016) simulated the dynamics of the WEC system using both coupled and decoupled models in the time domain. The coupled approach in DeepC was recommended to be used since the coupling effect was crucial for the fatigue damage analysis of the mooring line. The numerical model was validated by Yang et al. (2018) using the model tests of a taut-moored point-absorber type of WEC. Although some limitations were found when the wave conditions are close to the WEC's resonance frequency, the method demonstrated a good capability to simulate dynamic motions of the WEC system in most cases. Further validation for mooring tension was presented in Yang et al. (2021) considering both model and full-scale simulations.

Steel chain and wire rope have conventionally been used as the mooring lines, however, as operations move into more challenging marine environments, the offshore industry has repeatedly expressed concerns about the frequency of mooring line failures, potentially resulting in high-cost mooring designs (Bashir et al., 2017). Synthetic fibre ropes are potentially an enabling technology for the cost-effective design of MRE mooring systems (Weller et al., 2015). Some studies also show that the use of fibre ropes has the potential to reduce snap loads. A slack mooring and two-hybrid mooring systems for a WEC buoy were experimentally studied in Xu et al. (2020a,b) which showed that the snap load can frequently occur in the slack mooring system. Aiming to improve the knowledge of using elastic mooring lines for floating WECs, experimental study (Xu et al., 2018a) and numerical analysis (Xiang et al., 2018) of two mooring systems for WECs have been performed previously. It was found that the slack system, which contains the polyester component in mooring lines provides significantly lower spectral peaks. A detailed discussion of the performance of different synthetic ropes in the application for marine renewable energy devices was presented in Weller et al. (2015) and Wang et al. (2018), which concluded that polyester and nylon were considered as the suitable material for compliant mooring systems for WECs.

Many investigations regarding the time-dependent material behaviour of synthetic fibre ropes have been reported, such as Huang et al. (2015), Lian et al. (2018a,b, 2019, 2020), Wang et al. (2020), Xu et al. (2021a,b,c), however, the numerical dynamic analysis of the compliance mooring cables is still limited, as the material exhibit highly nonlinear and time-dependent load-elongation properties. The behaviour of a synthetic mooring system for the floating power plant wave energy converter was studied by Thomsen et al. (2016) using a quasi-static analysis, showing that the simple method underestimated the mooring tensions. Following the fibre rope mooring analysis procedure recommended by DNV (2015), Pham et al. (2019) proposed a practical procedure for numerical dynamic modelling of nylon ropes for a floating wind turbine with the empirical dynamic stiffness.

The objective of this work is to analyse and quantify the effects of dynamic stiffness on mooring systems composed of synthetic fibre ropes for WECs. Two mooring systems, composed of differed materials, are designed for a WEC installed off the coast of Portugal. The materials under examination are normally stiff polyester and wire-lay 3-strand nylon. It should be noted that the long-term cycling loading analysis is not considered in this study and it is assumed that the behaviour of the synthetic fibre ropes remains in the elastic domain.

For both systems, static and dynamic analysis in the time domain are carried out using the software DeepC, to determine the system response, as lines tensions and surge, pitch and heave motions of the point absorber wave energy converter. Two sets of analysis, considering three irregular operational sea states, are performed for each case of study. In the first set, the system responses are determined by applying a quasi-static stiffness model, using the nonlinear tension-elongation properties of the relative rope. Then, applying the mooring analysis procedures recommended by DNVGL-RP-E305 and Pham et al. (2019), the dynamic stiffness is calculated for each material and irregular sea state. At this point, the mooring analyses are carried out considering the static-dynamic stiffness model, and the responses of the system are defined and compared with the results obtained with the quasi-static stiffness model. The results presented show the importance of taking into account the dynamic stiffness for mooring analysis of systems composed of synthetic fibre rope materials. Indeed, for these cases of study, the quasi-static stiffness model underestimates the maximum mooring tensions by values that range between 30 and 40%. Moreover, in this work, the effects of the tension amplitude on the dynamic stiffness, and consequently on the system response, of nylon ropes are presented.

## 2. Methodology

### 2.1. Static-dynamic stiffness model

Synthetic fibre materials have become widely used in floating system applications because of their outstanding performances, such as corrosion resistance, low density, high strength to weight ratio, low installation costs and low-reliability risks.

Due to their viscous-elastic properties, synthetic fibre ropes do not present constant stiffness characteristics, as they vary with the load duration and amplitude, the number and frequency of load cycles, and the loading history (Fernandes et al., 1999). Engineers and classification societies have developed different models trying to represent the complex stiffness behaviour of these materials. One of the most recommended models that better reflects the basic elongation behaviour of polymer material, is the static-dynamic model. This model, based on numerous and rigorous research, allows to perform efficient and reliable mooring analysis, and if the parameters are properly determined, it yields a good approximation of lines tensions and vessel offset.

The macro-molecular structure of synthetic fibre materials has a strong influence on the elongation behaviour and the static-dynamic stiffness model is developed taking into account the morphology of these materials, which can be divided into a crystalline part and a non-crystalline part also called amorphous. When the tension member is loaded slowly, leaving the time for the crystalline and amorphous parts to react to the load, the resulting stiffness is a combination of the stiffness of both parts, and it is called static stiffness. However, when the tension member is subjected to cyclic loading, and the load cycle is not long enough to allow the amorphous part to react to the cyclic loading regime, all the load is taken by the crystalline part. The resultant stiffness, indicated as dynamic stiffness, is generally higher than the static stiffness, since the crystalline part is stiffer than the amorphous, and this results in a more rigid response of the rope (ABS, 2011).

The general idea of the static-dynamic stiffness model is to consider the static stiffness for the initial region of the loading curve, up to the mean tension, and then consider the dynamic stiffness to predict the response of the system to cyclic loads. This model tries to represent the actual condition of a mooring line in a real marine environment, which is typically subjected to a dynamic load that oscillates around a constant mean tension.

The stiffness of a rope can be expressed as:

$$EA = \frac{\Delta F}{\Delta \varepsilon} \tag{1}$$

where EA is the stiffness, $\Delta F$ is the change in load and $\Delta \varepsilon$ is the change in strain.

The non-dimensional stiffness (Kr) is defined as:

$$Kr = \frac{EA}{MBL} \tag{2}$$

where MBL is the minimum breaking strength of the cable.

The dynamic stiffness of synthetic fibre ropes has been widely investigated in recent years. Due to the numerous experiments and studies carried out, it has been possible to develop several empirical expressions to estimate the dynamic stiffness of different mooring materials. Generally, the dynamic stiffness of fibre ropes depends strongly on the mean tension, moderately on the tension amplitude and mildly on the frequency of loading (Del Vecchio, 1992).

Fernandes et al. (1999) proposed an empirical expression to estimate the dynamic stiffness of polyester ropes:

$$Krd = \alpha + \beta^{*}Lm - \gamma^{*}La + \delta^{*}\log(T_0) \tag{3}$$

where

- $\alpha, \beta, \gamma$ and $\delta$ are empirical coefficients.
- $Lm$ is the mean tension (% of MBL).
- $La$ is the tension amplitude (% of MBL).
- $T_0$ is the Loading period in seconds and can be assumed equal to the duration of the sea state.

Francois et al. (2000) demonstrated that loading frequency and tension amplitude have neglectable effects on the stiffness of polyester ropes and they proposed an empirical expression to calculate the dynamic stiffness of normally stiff polyester ropes that depends only on the mean tension:

$$Krd = 18.5 + 0.33^{*}Lm \tag{4}$$

On the other hand, experiments proved that nylon ropes tend to present a less linear behaviour, and for this material, the tension amplitude should be considered in the dynamic stiffness calculation, to do not underestimate the tension response.

Thus, Pham et al. (2019) proposed an empirical expression to calculate the dynamic stiffness of wire-lay 3-strand nylon rope:

$$Krd = a^{*}Lm - b^{*}La + c \tag{5}$$

where a, b, c are coefficients determined from multiple linear regression on the nylon dynamic stiffness testing data reported by Huntley (2016) and they are respectively 0.39, 0.21 and 2.08.

Xu et al. (2021) validated these empirical equations by performing model tests on polyester and nylon ropes. They concluded that Equations (4) and (5), with the relative coefficients presented above, showed good performance in predicting the dynamic stiffness of these types of synthetic fibre materials, with a relatively small error. Wang et al. (2020) experimentally tested different scales of a nylon rope with a diameter of 0.010 m. It was found that the dynamic stiffness for the sub rope which has a similar rope structure as the one used in Huntley (2016), agreed well with the empirical equation (5) using the coefficients 0.39, 0.21 and 2.08. Therefore, the empirical equations (4) and (5) of the dynamic stiffness are applied in the present study.

### 2.2. Mooring analysis procedure

The recent standard DNV (2015) and Falkenberg et al. (2017) proposed a practical mooring analysis procedure that considers the effect of dynamic stiffness of synthetic fibre ropes.

Procedure 1:

1. Perform the mooring static analysis using the appropriate non-linear working curves considering the mean environmental loads.
2. Determine the mean tension (Lm) at the fairlead, calculate the dynamic stiffness using Lm (Equation (4)) and update the model with this value of axial stiffness. A stress-free length of the lines corresponds to this stiffness and the mass per unit length of the lines are also updated.
3. Perform static and dynamic analysis with the updated mooring line properties.

However, this procedure ignores the tension amplitude effects, so it cannot be applied to nylon ropes and for this reason, in this study, it will be only considered for the dynamic modelling of polyester rope.

To consider the effects of the dynamic stiffness of nylon ropes on the mooring analysis of floating systems, Pham et al. (2019) proposed a practical procedure that takes into account La:

Procedure 2:

1. Same as Procedure 1.
2. Determine Lm at the fairlead and update the model with an axial stiffness determined by the empirical expression (Equation (5)) depending on Lm and an initial value of La (with the corresponding standard deviation $\sigma_1 = \frac{La}{\sqrt{2}}$) chosen optionally. A stress-free length of

**Table 1**
Main characteristics of the WEC system.

| | |
|---|---|
| Mass, $M_{WEC}$ [metric tonnes] | 268.42 |
| Draft, $D_{WEC}$ [m] | 15.265 |
| Centre of gravity ($x$, $y$, $z$), CoG [m][a] | (0, 0, −5.247) |
| Roll inertia relative to the motion reference point, $I_{xx}$ (kgm$^2$)[b] | $1.4902 \times 10^7$ |
| Pitch inertia relative to the motion reference point, $I_{yy}$ (kgm$^2$)[b] | $1.4902 \times 10^7$ |
| Yaw inertia relative to the motion reference point, $I_{zz}$ (kgm$^2$)[b] | $7.4411 \times 10^5$ |
| Centre of buoyancy ($x$, $y$, $z$), CoB [m][a] | (0, 0, −4.974) |
| Additional damping in the heave DoF, $B_{33}$ (kNs/m)[c] | 40.180 |
| Additional damping in the yaw DoF, $B_{66}$ (kNsm)[c] | 26.470 |

[a] The origin of the reference Cartesian coordinate is placed in the plane of water surface at the geometric centre of the WEC buoy when the buoy is in its still water condition.
[b] The motion reference point is defined at the geometric centre of the WEC buoy at its still-water plan, namely, the origin of the reference Cartesian coordinate.
[c] The additional damping is modelled as linear damping constant in either heave and yaw direction of the rigid body.

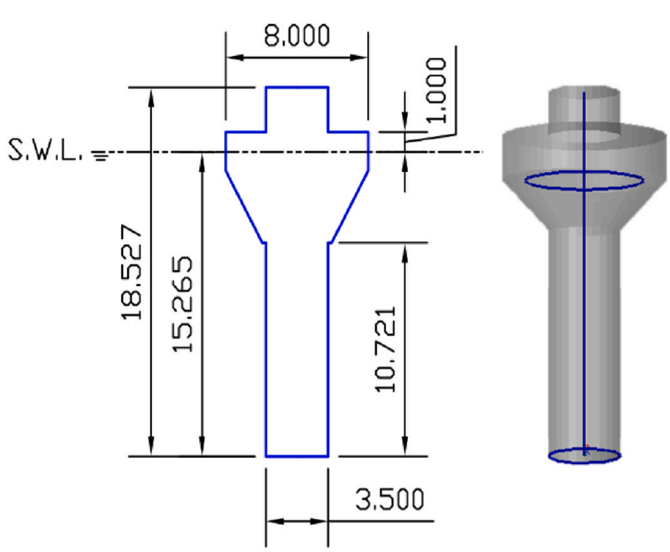


**Fig. 1.** Main dimensions of the WEC system.

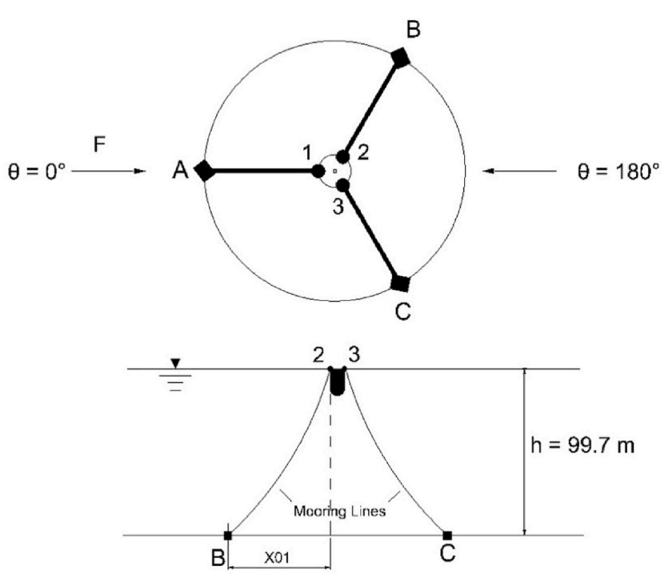


**Fig. 2.** WEC's mooring system configuration.

**Table 2**
Position of anchors and fairleads*.

| Fairleads coordinates | | | | Anchors coordinates | | | |
|---|---|---|---|---|---|---|---|
| Fairlead | x | y | z | Anchor | x | y | z |
| 1 | 4.0 | 0.0 | 0.0 | A | 103.0 | 0.0 | −99.7 |
| 2 | −2.0 | 3.5 | 0.0 | B | −51.5 | 89.2 | −99.7 |
| 3 | −2.0 | −3.5 | 0.0 | C | −51.5 | −89.2 | −99.7 |

**Table 3**
Materials characteristics.

| Material | Diameter (mm) | Submerged weight (kg/m) | Minimum Breaking Load (kN) | Pre-tension (kN) |
|---|---|---|---|---|
| Polyester | 52 | 0.52 | 831 | 40 |
| Nylon | 60 | 0.20 | 886 | 15 |

**Table 4**
Irregular sea states.

| Reference | Hs (m) | Tp (s) |
|---|---|---|
| OP1 | 1.5 | 6.5 |
| OP2 | 1.5 | 9 |
| OP3 | 1.5 | 11.5 |

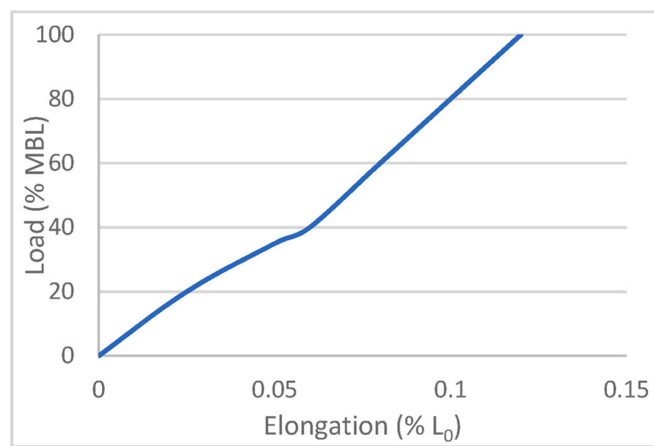


**Fig. 3.** Non-linear polyester working curves.

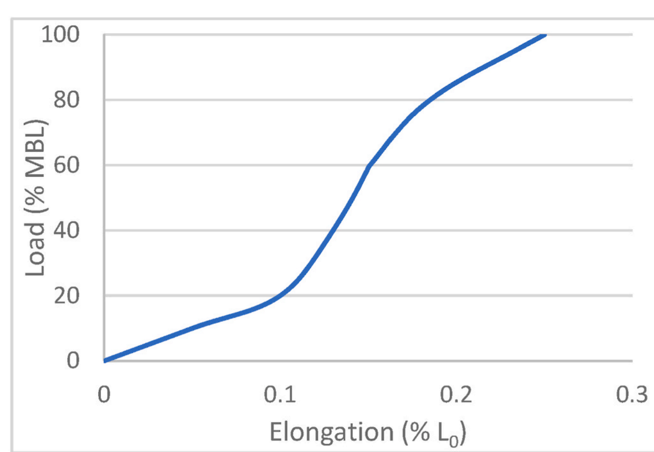


**Fig. 4.** Non-linear nylon working curves.

**Table 5**
Static tension results at fairlead (Lm).

| Case/ Condition | Case 1 | | | Case 2 | | |
|---|---|---|---|---|---|---|
| | OP1 | OP2 | OP3 | OP1 | OP2 | OP3 |
| Mean tension (kN) | 104 12.5% MBL | 101 12.2% MBL | 100 12.1% MBL | 91 10.2% MBL | 88 9.9% MBL | 97 9.8% MBL |

**Table 6**
Dynamic tensions of Case 1 calculated with the quasi-static stiffness model.

| Condition | Mean (kN) | Std (kN) | Min (kN) | Max (kN) |
|---|---|---|---|---|
| OP1 | 93.01 | 27.88 | 3.29 | 218.56 |
| OP2 | 90.11 | 30.31 | 3.11 | 208.68 |
| OP3 | 88.01 | 26.35 | 3.05 | 189.56 |

**Table 7**
Dynamic tensions of Case 1 calculated with the dynamic stiffness model.

| Condition | Axial stiffness (kN) | Mean (kN) | Std (kN) | Min (kN) | Max (kN) |
|---|---|---|---|---|---|
| OP1 | 18 796 | 92.35 | 62.46 | 2.01 | 369.50 |
| OP2 | 18 701 | 91.62 | 57.41 | 2.21 | 337.99 |
| OP3 | 18 678 | 89.14 | 46.51 | 1.02 | 283.91 |

the lines corresponds to this stiffness and the mass per unit length of the lines is also updated.

3. Perform static and dynamic analysis with the updated mooring line properties. Calculate the standard deviation $\sigma_2$ of the system response.
4. Check if the convergent criterion $\sigma_2 = \sigma_1$ is satisfied with a certain tolerance. If not, go back to step 2 and input a new tension amplitude La, and continue the procedure iteratively up to convergence.

The idea is to find a convergent dynamic stiffness for each sea state based on the empirical expressions (Equation (5)) for the specific mean tension and the convergent tension amplitude. The iterative process determines the convergent dynamic stiffness by comparing the standard deviation of the tension amplitude chosen optionally ($\sigma_1 = \frac{La}{\sqrt{2}}$) with the standard deviation of the tension response ($\sigma_2$).

The WEC motions and mooring dynamics are obtained by performing coupled dynamic analysis using the program DeepC, which is implemented in the commercial software SESAM (DNV, 2013c, 2021). The structural response of the mooring cables is solved through element discretisation with the FE method. In the simulation, the first-order bar elements are used to represent the mooring cables and all bar elements are assumed to be straight with a constant cross-sectional area along the element length (SINTEF, 2017). The deformation of the model allows for full rotations and translations in three-dimensional spaces. The coupled dynamic analysis approach using the DeepC program has been validated against model tests of a single-unit WEC system in Yang et al. (2018)

**Table 8**
WEC motions of Case 1 calculated with the quasi-static stiffness model.

| Condition/Motions | OP1 Lm = 12.5% MBL | | | | OP2 Lm = 12.2% MBL | | | | OP3 Lm = 12.1% MBL | | | |
|---|---|---|---|---|---|---|---|---|---|---|---|---|
| | Mean | Std | Min | Max | Mean | Std | Min | Max | Mean | Std | Min | Max |
| Surge (m) | −2.54 | 0.46 | −4.94 | −0.48 | −2.41 | 0.43 | −4.41 | −0.97 | −2.33 | 0.34 | −3.83 | −1.34 |
| Roll (m) | 0.00 | 0.00 | −0.01 | 0.03 | 0.00 | 0.00 | 0.00 | 0.01 | 0.00 | 0.00 | −0.01 | 0.01 |
| Sway (m) | 0.00 | 0.00 | −0.01 | 0.01 | 0.00 | 0.00 | 0.00 | 0.00 | 0.00 | 0.00 | 0.00 | 0.00 |
| Pitch (deg) | 2.72 | 2.45 | −6.75 | 12.3 | 2.61 | 3.61 | −9.77 | 14.97 | 2.50 | 3.83 | −10.67 | 15.87 |
| Heave (deg) | −0.27 | 0.36 | −1.57 | 1.03 | −0.27 | 0.35 | −1.67 | 1.05 | −0.26 | 0.34 | −1.51 | 0.97 |
| Yaw (deg) | 0.00 | 0.00 | −0.06 | 0.04 | 0.00 | 0.00 | −0.01 | 0.01 | 0.00 | 0.00 | −0.01 | 0.01 |

**Table 9**
WEC motions of Case 1 calculated with the dynamic stiffness model.

| Condition/Motions | OP1 Lm = 12.5% MBL | | | | OP2 Lm = 12.2% MBL | | | | OP3 Lm = 12.1% MBL | | | |
|---|---|---|---|---|---|---|---|---|---|---|---|---|
| | Mean | Std | Min | Max | Mean | Std | Min | Max | Mean | Std | Min | Max |
| Surge (m) | −1.99 | 0.36 | −3.55 | −0.49 | −1.74 | 0.31 | −2.73 | −0.42 | −1.74 | 0.23 | −2.60 | −0.79 |
| Roll (m) | 0.00 | 0.00 | −0.01 | 0.00 | 0.00 | 0.00 | 0.00 | 0.01 | 0.00 | 0.00 | −0.01 | 0.00 |
| Sway (m) | 0.00 | 0.00 | 0.00 | 0.00 | 0.00 | 0.00 | 0.00 | 0.00 | 0.00 | 0.00 | 00.00 | 0.00 |
| Pitch (deg) | 3.00 | 2.92 | −7.22 | 15.83 | 2.82 | 3.55 | −9.00 | 17.98 | 2.66 | 3.55 | −8.46 | 15.29 |
| Heave (deg) | −0.26 | 0.27 | −1.50 | 0.74 | −0.27 | 0.27 | −1.36 | 0.78 | −0.27 | 0.29 | −1.37 | 0.74 |
| Yaw (deg) | 0.00 | 0.00 | −0.03 | 0.04 | 0.00 | 0.00 | −0.02 | 0.02 | 0.00 | 0.00 | −0.01 | 0.01 |

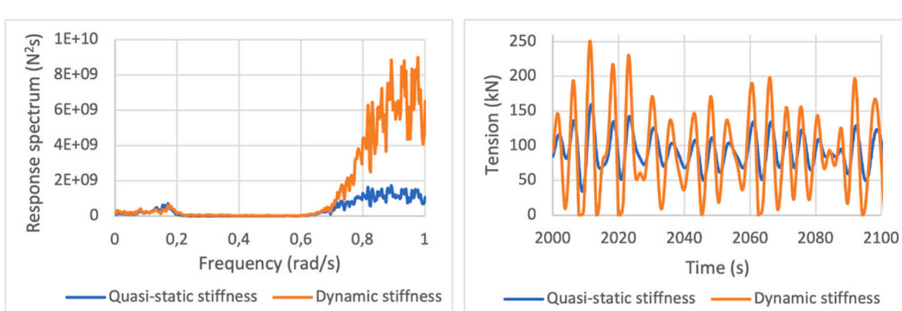


a: Tension spectral density b: Tension time series

**Fig. 5.** Comparison of tension response between stiffness models for Case 1 under irregular condition OP1.

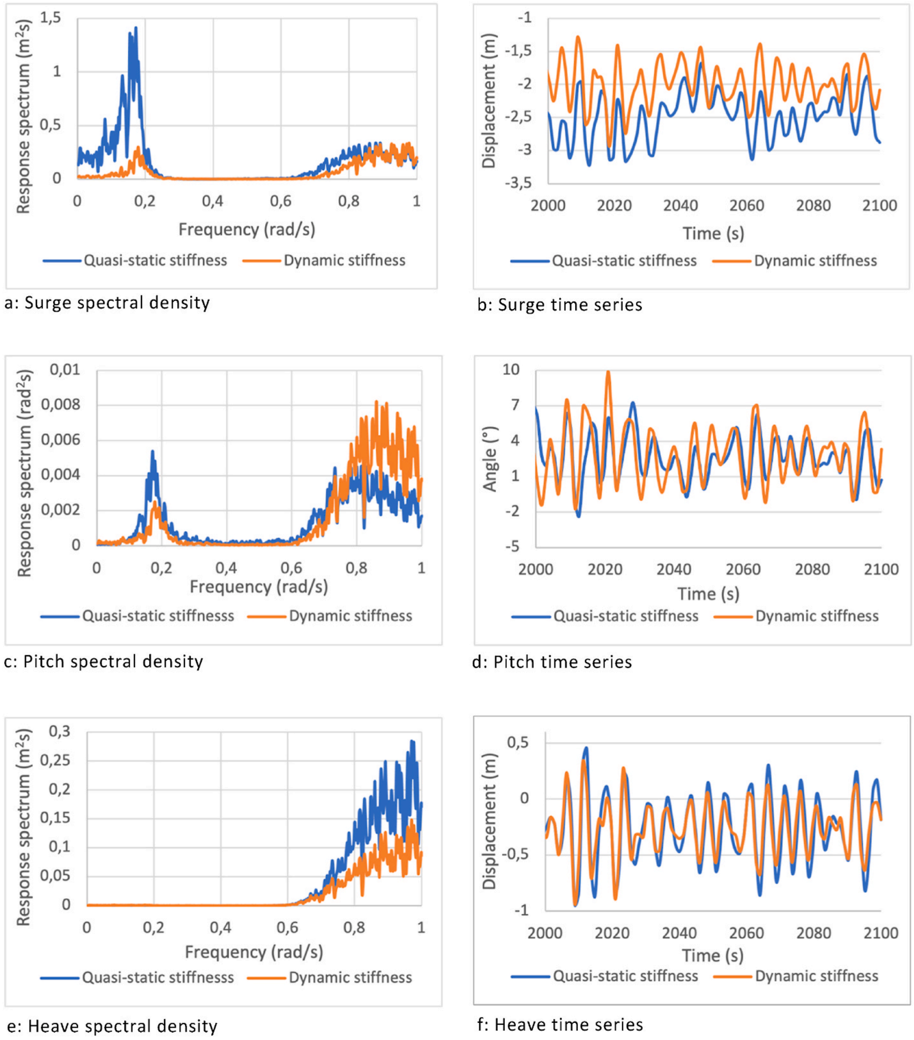


**Fig. 6.** Comparison of WEC motions between stiffness models for Case 1 under irregular condition OP1.

**Table 10**
Step of iteration for Case 2 and OP1.

| Iteration step | Lm (% MBL) | La (% MBL) | Axial stiffness (kN) | Std 1 $\left(\sigma_1 = \frac{La}{\sqrt{2}}\right)$ (kN) | Std 2 Tension Response $\sigma_2$ (kN) | Difference Between $\sigma_1$ and $\sigma_2$ (%) |
|---|---|---|---|---|---|---|
| 1 | 10.20 | 10.20 | 3472 | 63.98 | 15.97 | 300.7 |
| 2 | 10.20 | 5.00 | 4442 | 31.33 | 19.69 | 59.1 |
| 3 | 10.20 | 3.35 | 4749 | 20.99 | 20.82 | 0.8 |

regarding WEC motions, in Yang et al. (2020) regarding mooring forces and of a semi-submersible platform in Xu et al. (2018b) regarding body motions and mooring forces.

## 3. Model description

### 3.1. WEC characteristic

The mooring systems analysed in this study are designed for the prototype concept WaveEL 3.0, which was developed by the Swedish company Waves4Power and the location chosen for the installation is a site off the coast of Figueira da Foz, Portugal. This location is characterized by a water depth equal to 99.7 m. In Table 1 and Fig. 1 are reported the main dimensions of the floating body, a point absorber WEC type, which harvests incoming wave-energy from all directions. The system takes advantage of the heave motion to generate electricity and the PTO mechanism is realised by water movement inside a central hollow tube of the floating device. The same WEC system was installed in Runde (Norway) 2017 and it showed an installed power performance of 125 kW, according to Waves4Power (2018). The WEC was investigated by Yang et al. (2018) regarding its energy performance and the methods to simulate and assess the fatigue characteristics of mooring lines. Moreover, experiments and numerical investigations were conducted on the buoy motions (Yang et al., 2018) and the mooring line forces (Yang et al., 2021). In this study, the effects of dynamic stiffness of elastic moorings on the buoy motions and mooring tensions are analysed and quantified.

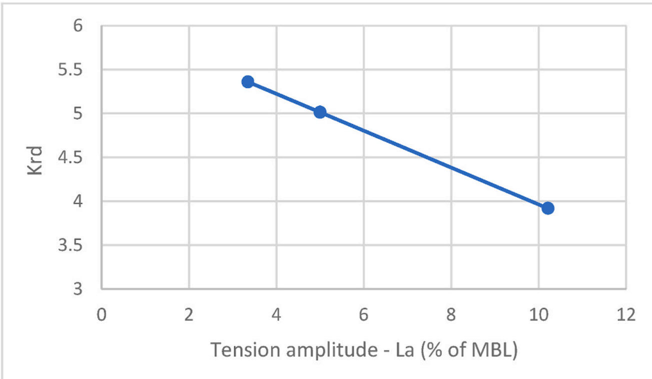


**Fig. 7.** Effect of the tension amplitude (La) on the dynamic stiffness of nylon rope.

**Table 11**
Dynamic tensions of Case 2 and condition OP1, calculated varying La.

| Iteration step | Lm (% MBL) | La (% MBL) | Axial stiffness (kN) | Mean (kN) | Std (kN) | Min (kN) | Max (kN) |
|---|---|---|---|---|---|---|---|
| 1 | 10.20 | 10.20 | 3472 | 77.20 | 15.97 | 20.90 | 168.39 |
| 2 | 10.20 | 5.00 | 4442 | 76.84 | 19.69 | 7.56 | 183.03 |
| 3 | 10.20 | 3.35 | 4749 | 77.34 | 20.82 | 4.84 | 187.13 |

### 3.2. Mooring system

As shown in Fig. 2, a taut three-leg mooring system is designed for the WEC system, where F indicates the direction of the external forces acting on the floating body, A, B, C are the positions of the anchors and 1,2,3 the position of the fairleads. In this study two mooring systems composed of different materials are considered and analysed:

**Case 1.** Mooring lines composed of normally stiff polyester ropes.

**Case 2.** Mooring lines composed of wire-lay 3-strand nylon ropes.

The configurations are characterized by three equal taut mooring legs symmetrically placed, anchored to the seabed with gravity anchors, and for both cases, the length of the lines is equal to 140 m. The diameter of the lines has been chosen from the (Bridon), in such a way that the two systems would present similar minimum breaking load (MBL) (Table 3). The gravity anchors have a mass of 40 tons and are designed to be spacially fixed. For this reason, in the numerical model, the anchor points are represented as six-DoF fixed points. More detailed information on the mooring system characteristics, such as the position of the anchors and materials properties, are reported in Tables 2 and 3.

### 3.3. Environmental condition

The mooring systems are tested in 3 operational irregular sea states performing static and dynamic coupled analysis in the time domain, using the FEM program DeepC. The dynamic simulations have a duration of 3 h and the incident wave direction is parallel to one mooring leg. The irregular wave conditions chosen have a high probability of occurrence according to the scatter diagram presented by Silva et al. (2015, 2016, 2018), and their characteristics are reported in Table 4.

The spectrum model used to describe the irregular sea state is the JONSWAP spectrum and the density energy E(f), can be calculated from the significant wave height ($H_S$) and the peak frequency ($\omega p = 1/T_p$) as:

$$E(f) = a * g^2 * \omega^{-5} * exp\left[-B * \left(\frac{\omega p}{\omega}\right)^4\right] * \gamma^{exp\left[-\frac{(\omega-\omega p)^2}{2*\sigma^2*\omega p^2}\right]} \tag{6}$$

where:

- $a = 1.2905 * H_S{}^2/T_P{}^4$.
- g is the gravitational acceleration.
- $\omega$ is the frequency.
- $\omega p$ is the peak frequency.
- $B = 1.25$.
- $\gamma$ is the peak-enhancement factor, in this case, equal to 1.
- $\sigma = 0.07$ for $\omega > \omega p$.
- $\sigma = 0.0$ for $\omega < \omega p$.

Moreover, a current characterized by a constant speed of 2 m/s, no

**Table 12**
WEC motions of Case 2 and condition OP1, calculated varying La.

| Condition/Motions | 1 – La = 10.2% of MBL | | | | 2 – La = 5% of MBL | | | | 3 – La = 3.35% of MBL | | | |
|---|---|---|---|---|---|---|---|---|---|---|---|---|
| | Mean | Std | Min | Max | Mean | Std | Min | Max | Mean | Std | Min | Max |
| Surge (m) | −7.23 | 0.60 | −10.89 | −4.98 | −7.15 | 0.56 | −10.45 | −5.27 | −7.94 | 0.55 | −10.15 | −5.13 |
| Roll (m) | 0.00 | 0.00 | −0.01 | 0.02 | 0.00 | 0.00 | −0.01 | 0.02 | 0.00 | 0.00 | −0.02 | 0.03 |
| Sway (m) | 0.00 | 0.00 | 0.00 | 0.01 | 0.00 | 0.00 | 0.00 | 0.01 | 0.00 | 0.00 | −0.01 | 0.01 |
| Pitch (deg) | 2.90 | 1.98 | −6.07 | 12.25 | 3.00 | 2.10 | −5.88 | 12.48 | 2.98 | 2.14 | −5.77 | 12.56 |
| Heave (deg) | −0.20 | 0.40 | −1.68 | 1.25 | −0.19 | 0.39 | −1.66 | 1.24 | −0.20 | 0.39 | −1.65 | 1.24 |
| Yaw (deg) | 0.00 | 0.00 | −0.07 | 0.03 | 0.00 | 0.00 | −0.10 | 0.03 | 0.00 | 0.00 | −0.01 | 0.01 |

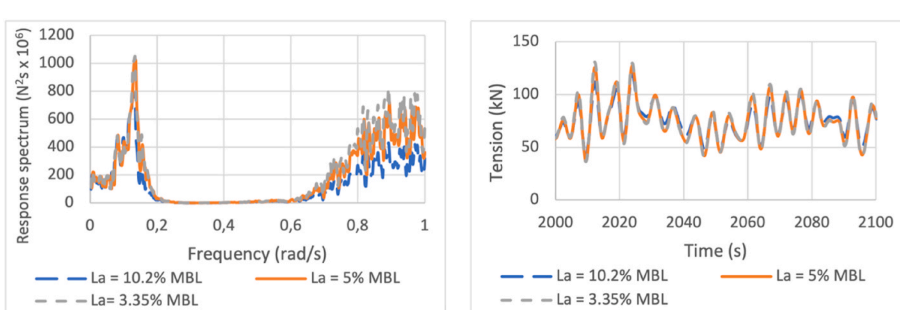


a: Tension spectral density b: Tension time series

**Fig. 8.** Comparison of tension response between different stiffness cases (La) under irregular condition OP1.

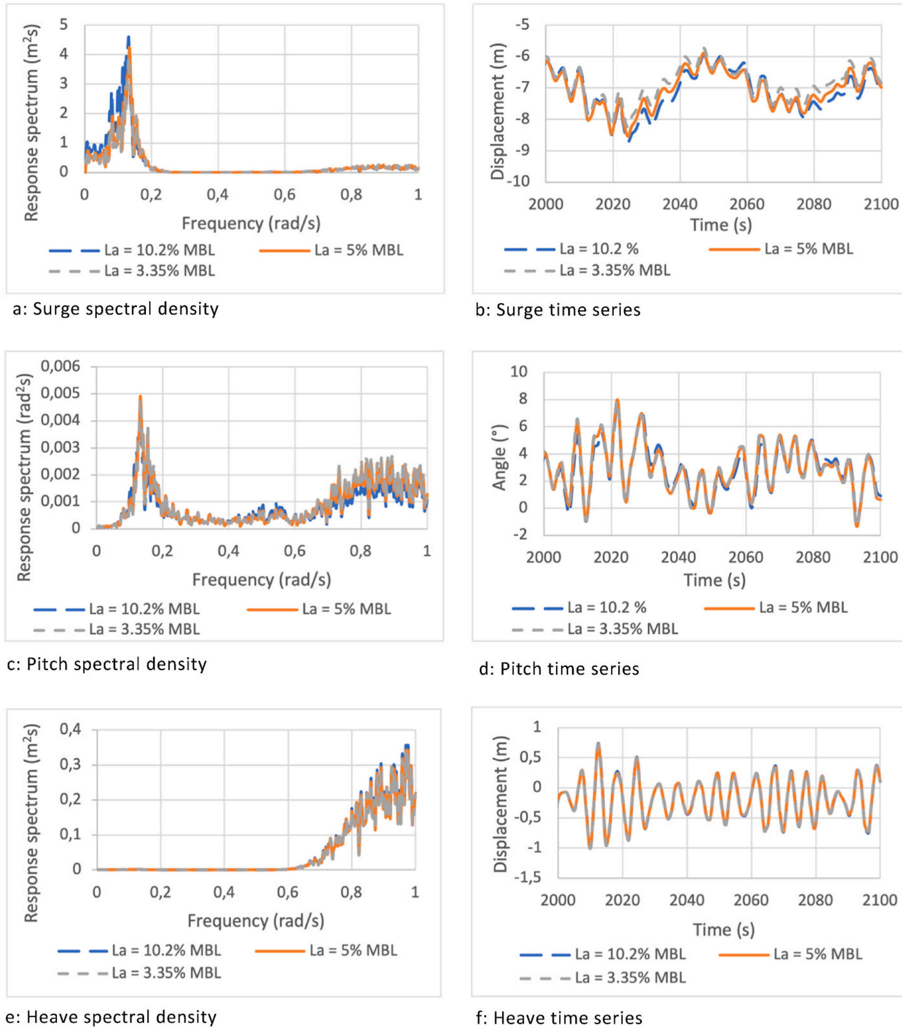


**Fig. 9.** Comparison of WEC motions between different stiffness cases (La) under irregular condition OP1.

**Table 13**
Dynamic tensions of Case 2 calculated with the quasi-static stiffness model.

| Condition | Mean (kN) | Std (kN) | Min (kN) | Max (kN) |
|---|---|---|---|---|
| OP1 | 75.48 | 9.75 | 41.73 | 133.64 |
| OP2 | 72.67 | 8.82 | 40.62 | 112.32 |
| OP3 | 71.12 | 8.20 | 39.96 | 106.57 |

**Table 14**
Dynamic tensions of Case 2 calculated with the dynamic stiffness model.

| Condition | Lm (% MBL) | Convergent La (% MBL) | Axial stiffness (kN) | Mean (kN) | Std (kN) | Min (kN) | Max (kN) |
|---|---|---|---|---|---|---|---|
| OP1 | 10.2 | 3.35 | 4749 | 77.34 | 20.82 | 4.84 | 187.13 |
| OP2 | 9.9 | 3.40 | 4639 | 73.84 | 21.31 | 6.43 | 170.02 |
| OP3 | 9.8 | 3.12 | 4653 | 71.62 | 19.59 | 3.61 | 155.58 |

**Table 15**
WEC motions of Case 2 calculated with the quasi-static stiffness model.

| Condition/Motions | OP1 Lm = 10.2% MBL | | | | OP2 Lm = 9.9% MBL | | | | OP3 Lm = 9.8% MBL | | | |
|---|---|---|---|---|---|---|---|---|---|---|---|---|
| | Mean | Std | Min | Max | Mean | Std | Min | Max | Mean | Std | Min | Max |
| Surge (m) | −8.63 | 0.72 | −13.28 | −6.16 | −8.27 | 0.48 | −10.78 | −6.96 | −8.07 | 0.39 | −10.15 | −6.92 |
| Roll (m) | 0.00 | 0.00 | −0.01 | 0.01 | 0.00 | 0.00 | −0.01 | 0.01 | 0.00 | 0.00 | −0.01 | 0.01 |
| Sway (m) | 0.00 | 0.00 | 0.00 | 0.00 | 0.00 | 0.00 | 0.00 | 0.00 | 0.00 | 0.00 | 0.00 | 0.00 |
| Pitch (deg) | 2.65 | 1.74 | −6.09 | 11.75 | 2.53 | 2.31 | −7.15 | 10.76 | 2.47 | 3.10 | −8.18 | 12.57 |
| Heave (deg) | −0.19 | 0.41 | −1.66 | 1.25 | −0.19 | 0.40 | −1.57 | 1.30 | −0.19 | 0.38 | −1.63 | 1.19 |
| Yaw (deg) | 0.00 | 0.00 | −0.01 | 0.01 | 0.00 | 0.00 | 0.00 | 0.01 | 0.00 | 0.00 | 0.00 | 0.01 |

**Table 16**
WEC motions of Case 2 calculated with the dynamic stiffness model.

| Condition/Motions | OP1 Lm = 10.2% - La = 3.35% MBL | | | | OP2 Lm = 9.9% - La = 3.40 %MBL | | | | OP3 Lm = 9.8% - La = 3.12% MBL | | | |
|---|---|---|---|---|---|---|---|---|---|---|---|---|
| | Mean | Std | Min | Max | Mean | Std | Min | Max | Mean | Std | Min | Max |
| Surge (m) | −7.94 | 0.55 | −10.15 | −5.13 | −6.82 | 0.44 | −8.98 | −5.49 | −6.68 | 0.36 | −8.28 | −5.44 |
| Roll (m) | 0.00 | 0.00 | −0.02 | 0.03 | 0.00 | 0.00 | −0.01 | 0.01 | 0.00 | 0.00 | −0.01 | 0.01 |
| Sway (m) | 0.00 | 0.00 | −0.01 | 0.01 | 0.00 | 0.00 | 0.00 | 0.00 | 0.00 | 0.00 | −0.01 | 0.00 |
| Pitch (deg) | 2.98 | 2.14 | −5.77 | 12.56 | 2.84 | 3.16 | −9.94 | 13.89 | 2.75 | 3.87 | −9.99 | 15.73 |
| Heave (deg) | −0.20 | 0.39 | −1.65 | 1.24 | −0.19 | 0.37 | −1.63 | 1.23 | −0.19 | 0.36 | −1.56 | 1.11 |
| Yaw (deg) | 0.00 | 0.00 | −0.01 | 0.01 | 0.00 | 0.00 | −0.04 | 0.02 | 0.00 | 0.00 | −0.06 | 0.04 |

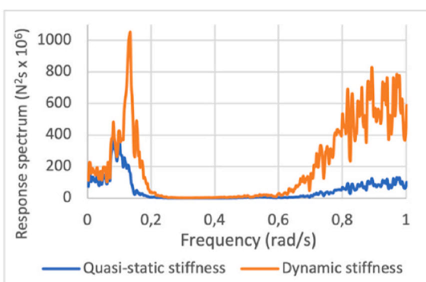

a: Tension spectral density

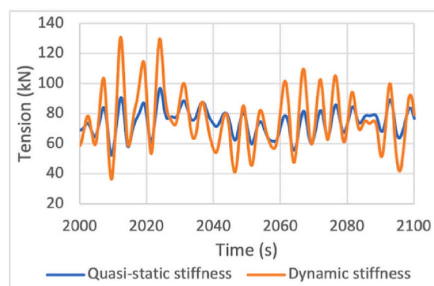

b: Tension time series

**Fig. 10.** Comparison of tension response between stiffness models for Case 2 under irregular condition OP1.

vertical gradient and the same direction of the incident waves are acting on the system in each environmental condition. For simplification, no wind loads are applied, and the current loads are approximated to a steady contribution and included in the mean tension.

## 4. Results and discussions

As the first step, the non-linear tension elongation relations (working curves) need to be determined. In this study, the worked tension elongation curves are taken from the Bridon fibre rope catalogue, and they are presented in Figs. 3 and 4 for polyester and nylon respectively.

First, static and dynamic analyses are performed applying the quasi-static stiffness model and using the relative tension-elongation curve, without considering the dynamic stiffness effects on the system response. From the static analysis, the mean tensions (Lm) for each specific environmental condition are defined. The results obtained are reported in Table 5, and they will be used later to estimate the dynamic stiffness of the relative rope. The dynamic analysis results, such as WEC motions and tensions at the fairlead of the most loaded line, are reported in Tables 6 and 8 for Case 1 and Tables 13 and 15 for Case 2. The idea is to compare these results with the values that will be obtained applying the mooring analysis procedures explained previously which take into account the axial dynamic stiffness. Thus, it will be possible to analyse and quantify the effects of dynamic stiffness on the system response.

### 4.1. Polyester

Following procedure 1, WEC motions and dynamic tensions of the lines are calculated with the dynamic stiffness of polyester ropes taking into account. Using Lm calculated previously and reported in Table 5, the values of the axial dynamic stiffness of each sea state can be obtained directly by applying Equation (4). Finally, static and dynamic coupled analyses are performed with the updated mooring lines properties and the results are reported in Tables 7 and 9.

Comparing the results obtained with the two stiffness models, it is observed that for polyester ropes maximum tension results are between 30 and 40% higher when the dynamic stiffness is considered. This result is confirmed in Fig. 5a and b where the spectral density and the time history of the tension at the fairlead of both stiffness models are compared respectively, for the irregular condition OP1. Indeed, tension responses obtained with the dynamic stiffness model presents higher oscillations over the time of the dynamic simulation and more severe responses, for both peaks and through values.

Moreover, it is observed in Fig. 5a that the mooring tensions present two peaks. The first one, around 0.2 rad/s, is close to the surge resonance frequency of the system and presents similar tension results for the two stiffness models. The second peak, which is around 0.9 rad/s (in correspondence with the heave resonance frequency), presents measured tensions characterized by higher values and a greater difference

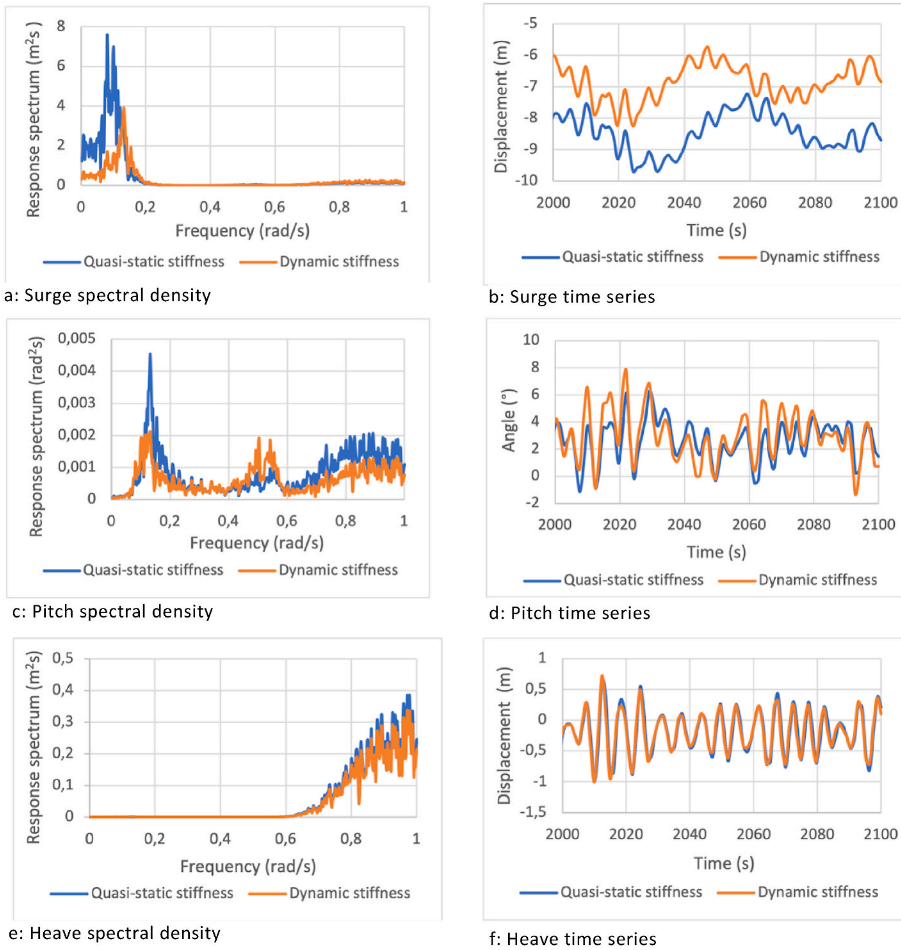


**Fig. 11.** Comparison of WEC motions between stiffness models for Case 2 under irregular condition OP1.

between the two stiffness models (quasi-static and dynamic). Therefore, from these results, it appears that the dynamic stiffness of polyester rope has a greater impact on mooring tensions in the higher frequency region.

From the results of the motions presented in Tables 8 and 9, it is observed that the predominant motions are surge, pitch and heave. This happens because the direction of current and incoming waves is parallel to the x-direction. Moreover, all WEC motions present smaller peak values when calculated with the dynamic stiffness model, except for pitch motion. In Fig. 6, the response spectrums and time series of surge, pitch and heave motions are reported. Results show that for surge motion the quasi-static stiffness model presents a greater value in the low-frequency region (0–0.3 rad/s) compared to the dynamic stiffness model, but similar results in the rest of the frequency domain. It is found that the variation of pitch motion is similar to the results of surge motion, for frequency smaller than 0.3 rad/s and to the results of heave motion for frequency greater to 0.7 rad/s. Pitch motion shows higher peak values for the dynamic stiffness case, which occurs between 0.7 and 1 rad/s, while in the low-frequency region, quasi-static results are higher. Finally, Fig. 5e and f shows that heave motion is generally smaller for the dynamic stiffness case.

### 4.2. Nylon

As mentioned before, the dynamic stiffness of nylon rope is not only dependent on the mean tension, but also the tension amplitude. For this reason, the iterative procedure described previously (procedure 2), needs to be carried out to determine the convergent dynamic stiffness, for each specific sea state. The procedure starts with the first value of La chosen equal to Lm, which is the lowest realistic stiffness case, according to Pham et al. (2019). The steps of the procedure, carried out for condition OP1, are presented in Table 10, and it is possible to notice that for this case the convergency is reached after 3 iterations.

For all the irregular conditions considered in this study, the iterative process stops when the difference between the standard deviation calculated from La as $\sigma_1 = \frac{La}{\sqrt{2}}$ and the measured standard deviation of the tension response is below 1%. Moreover, in Fig. 7 it is possible to observe the impact of La on the axial dynamic stiffness of the mooring system.

To understand the effects of La on the system response, Tables 11 and 12 compare tensions and WEC motion statistics of different dynamic stiffness cases. It is possible to notice that the same Lm and a lower La results in a stiffer rope, which implies higher tension responses in the lines, around 10%, from the greater to the lower value of La. Moreover, decreasing La smaller WEC motions are measured, except for pitch motion which shows a small increment.

The spectral density and the time series of the measured tension at the fairlead of the up-loaded line are shown in Fig. 8a and b respectively. These graphs confirm that higher amplitude loads result in lower tension responses, in both peaks and throughs, throughout the whole frequency domain. The spectral density and time series of the surge, pitch, and heave calculated with different La are compared in Fig. 9. Results show that higher stiffness cases (La = 3.35) correspond to smaller WEC motions, except for pitch motions which present an opposite behaviour.

Following the same procedure, a convergent dynamic stiffness is found for each specific irregular condition. Tables 14 and 16 show respectively the tension and the WEC motion statistics relative to the final step of this iterative process, performed for each irregular sea state.

These values can be compared with results presented in Tables 13 and 15 where the dynamic results obtained previously with the quasi-static stiffness model are reported, without considering the effects of dynamic stiffness.

Comparing the results of the maximum tension obtained using the quasi-static stiffness model (Table 13) and the dynamic stiffness model (Table 14), it can be observed that the first model presents peak values around 30% smaller. These results confirmed that for nylon as for polyester ropes, the mooring analysis performed with the quasi-static model tends to underestimate the peak values of tension, and this could lead to an under-dimensioning of the mooring lines.

The spectral density and effective tension time series of Case 2 are reported in Fig. 10 by using the two stiffness models, quasi-static and dynamic. Differently from the polyester case, for the nylon case, the maximum values of tension are registered in the lower frequency region, in correspondence with the surge natural frequency. The same consideration can be made observing Figs. 6c and 11c where the pitch motion spectral density of polyester and nylon case are reported respectively. For the polyester case, pitch motion presents bigger values in the high-frequency region, around the heave natural frequency, while for the nylon case, the greater response values are measured in the lower frequency region.

Moreover, comparing the results obtained from the polyester and the nylon mooring systems, it can be seen that polyester is characterized by higher stiffness values. Consequently, this results in more restricted values of motions in all directions and consequently, higher tension responses in the lines. This underlines the advantages of using nylon ropes to reduce maximum mooring tensions and increase the motion of the WEC system. As mentioned before the WEC under examination is a point absorber type and takes advantage of the heave motion to generate electricity. Nylon ropes would ensure greater values of heave motion which means a higher energy conversion efficiency.

## 5. Conclusions

The effects of dynamic axial stiffness of elastic moorings on the dynamic behaviour of a floating point-absorber WEC are investigated in this study. Two mooring systems, composed of polyester and nylon ropes, are analysed. Using the FEM software DeepC, dynamic coupled analyses in the time domain are carried out to determine mooring tensions and the response of the system under different irregular conditions. Two different analyses were performed using the program to identify the effects of the dynamic stiffness. By using the non-linear stiffness working curves of the ropes, namely, the quasi-static stiffness model, the WEC motions and line tensions are estimated firstly. Secondly, the dynamic stiffness of the ropes is calculated according to the available empirical equations, and static and dynamic analyses of the moored WEC systems are carried out following the practical procedures, depending on the type of the rope. For nylon ropes, an iterative process presented that takes into account the tension amplitude is carried out.

The comparisons of the numerical results between the two analyses show the importance of accounting for the dynamic stiffness of both polyester and nylon ropes. For this specific case of study, the maximum tensions estimated with the quasi-static stiffness model are 30–40% lower. Dynamic results also demonstrate the significance of the load amplitude (La) when calculating the dynamic stiffness of nylon ropes. For instance, the results of the mooring tension obtained from the cases of La = 10.2% MBL and of La = 3.35% MBL, show a 10% difference in the peak values.

In addition, the results also show that, for the studied WEC system, the nylon rope shows advantages over polyester, because of the lower maximum mooring tensions and higher WEC motions when the mooring configuration is the same.

However, prototype tests of the real mooring system and the ropes should be carried out to validate the models applied in this study and understand the accuracy of the mooring procedures of both polyester and nylon ropes. Moreover, due to the low number of studies and research, analysis on the fatigue failures of these synthetic materials, especially nylon, could help to increase the knowledge on these materials and they would be interesting topics for future works.

## CRediT authorship contribution statement

**Francesco Depalo:** Methodology, Formal analysis, Writing – original draft, Visualization. **Shan Wang:** Methodology, Writing – original draft. **C. Guedes Soares:** Writing – review & editing, Supervision. **Shun-Han Yang:** Writing – review & editing. **Jonas W. Ringsberg:** Writing – review & editing.

## Declaration of competing interest

The authors declare that they have no known competing financial interests or personal relationships that could have appeared to influence the work reported in this paper.

## Acknowledgement

This work was financially supported by the Project "ELASTMOOR - Elastic mooring systems for wave energy converters" which is co-funded by European Union's Horizon 2020 research and innovation programme under the framework of OCEANERA-NET (http://oceaneranet.eu) and by the Portuguese Foundation for Science and Technology (Fundação para a Ciência e Tecnologia - FCT) under contract (OCEANERA/0006/2016). The work contributes to the Strategic Research Plan of the Centre for Marine Technology and Ocean Engineering (CENTEC), which is financed by FCT under contract UIDB/UIDP/00134/2020.

## References

ABS, 2011. Guidance Notes on the Application of Fiber Rope for Offshore Mooring. ABS 90-2011.
Amaechi, C.V., Wang, F., Hou, X., Ye, J., 2019. Strength of submarine hoses in Chinese-lantern configuration from hydrodynamic loads on CALM buoy. Ocean Eng. 1 (171), 429–442.
American Petroleum Institute (API), 2005. API-RP-2SK: Design and Analysis of Stationkeeping Systems for Floating Structures. American Petroleum Institute, Washington, DC, USA.
Bridon. Fibre rope catalogue. http://www.lisintertrade.com/image/PDF/bridon%20fibre%20rope%20catalogue.pdf.
Bashir, I., Walsh, J., Thies, P.R., Weller, S.D., Blondel, P., Johanning, L., 2017. Underwater acoustic emission monitoring–Experimental investigations and acoustic signature recognition of synthetic mooring ropes. Appl. Acoust. 121, 95–103.
Bergdahl, L., Kofoed, J.P., 2015. Simplified Design Procedures for Moorings of Wave-Energy Converters: Deliverable, 2.2. DCE Technical reports No, p. 172.
Chakrabarti, S.K., 2005. Handbook of Offshore Engineering. Elsevier.
Cruz, J., 2007. Ocean Wave Energy: Current Status and Future Perspectives. Springer Science & Business Media.
Cribbs, A.R., Kärrsten, G.R., Shelton, J.T., Nicoll, R.S., Stewart, W.P., 2017. Mooring System Considerations for Renewable Energy Standards. Offshore Technol. Conf., OTC, Houston, Texas, USA.
Czech, B., Bauer, P., 2012. Wave energy converter concepts: design challenges and classification. In: IEEE Industrial Electronics Magazine, 6, pp. 4–16, 2.
Davidson, J., Ringwood, J.V., 2017. Mathematical modelling of mooring systems for wave energy converters—a review. Energies 10 (5), 666.
Del Vecchio, C.J.M., 1992. Light Weight Material for Deepwater Mooring. PhD thesis. University of Reading.
Depalo, F., Wang, S., Xu, S., Guedes Soares, C., 2021. Design and analysis of a mooring system for a wave energy converter. J. Mar. Sci. Eng. 9 (7), 782.
DNV, 2004. DeepC – Deep Water Coupled Analysis Tool. A White Paper Rev3. Det Norske Veritas (DNV), Høvik, Norway.
DNV, 2013a. SesamDeepC, V5.0-06. Det Norske Veritas(DNV), Høvik, Norway.
DNV, 2013b. RIFLEX User Manual Version 4.0 Rev3. Detnorske Veritas (DNV), Høvik, Norway.
DNV, 2013c. Sesam HydroD V4.7-01. Det Norske Veritas(DNV), Høvik, Norway.
DNV, 2015. Recommended Practice DNVGL-RP-E305, Det Norske Veritas(DNV),Høvik, Norway.
DNV, 2018. Offshore Standards DNV-OS-E301, Det Norske Veritas(DNV),Høvik,Norway.
DNV, 2021. Sesam Feature Description, Det Norske Veritas(DNV),Høvik,Norway.
Doyle, S., Aggidis, G.A., 2019. Development of multi-oscillating water columns as wave energy converters. Renew. Sustain. Energy Rev. 1 (107), 75–86.
Falkenberg, E., Ahiem, V., Yang, L., 2017. Best Practice for Analysis of Polyester Rope Mooring Systems. Offshore Technology Conference, OTC-27761-MS.

Francois, M., Davies, P., 2000. Fibre Rope for Deepwaer Mooring: a Practical Model for the Analysis of Polyester Mooring Systems. Proceeding of Rio Oil and Gas conference Rio de Janeiro.
Fernandes, A.C., Del Vecchio, C.J.M., Castro, G.A.V., 1999. Mechanical properties of polyester mooring cables. Int. J. Offshore Polar Eng. 208–213.
Fitzgerald, J., 2009. Position Mooring of Wave Energy Converters. PhD Thesis. Chalmers University of Technology, Gothenburg, Sweden.
Giannini, G., Rosa-Santos, P., Ramos, V., Taveira-Pinto, F., 2020. On the development of an offshore version of the CECO wave energy converter. Energies 13, 1036.
Guedes Soares, C., Bhattacharjee, J., Tello, M., Pietra, L., 2012. In: Guedes Soares, C., Garbatov, Y., Sutulo, S., Santos, T.A. (Eds.), Review and Classification of Wave Energy Converters, Maritime Engineering and Technology. Taylor & Francis Group, London, UK, pp. 585–594.
Huang, W., Liu, H., Lian, Y., Li, L., 2015. Modeling nonlinear time-dependent behaviors of synthetic fiber ropes under cyclic loading. Ocean Eng. 109, 207–216.
Huntley, M.B., 2016. Fatigue and modulus characteristics of wire-lay nylon rope. OCEANS 2016 MTS/IEEE monterey. OCE 5–10, 2016.
ISO, 2013. ISO 19901-7 2005: Stationkeeping Systems for Floating Offshore Structures and Mobile Offshore Units. International Organization for Standardization, Geneva, Switzerland.
Johanning, L., Smith, G.H., Wolfram, J., 2006a. Mooring design approach for wave energy converters. Proc. Inst. Mech. Eng. Part M J. Eng. Marit. Environ. 220, 159–174.
Johanning, L., Smith, G.H., Wolfram, J., 2006b. Mooring design approach for wave energy converters. Proc. IME M J. Eng. Marit. Environ. 220 (4), 159–174.
Lian, Y., Liu, H., Li, L., Zhang, Y., 2018a. An experimental investigation on the bedding-in behavior of synthetic fiber ropes. Ocean Eng. 160, 368–381.
Lian, Y., Liu, H., Yim, S.C., Zheng, J., Xu, P., 2019. An investigation on internal damping behavior of fiber rope. Ocean Eng. 182, 512–526.
Lian, Y., Yim, S.C., Zheng, J., Liu, H., Zhang, N., 2020. Effects of damaged fiber ropes on the performance of a hybrid taut-wire mooring system. J. Offshore Mech. Arctic Eng.,142(1),, 011607.
Lian, Y., Zheng, J., Liu, H., Xu, P., Gan, L., 2018b. A study of the creep-rupture behavior of HMPE ropes using viscoelastic-viscoplastic-viscodamage modeling. Ocean Eng. 162, 43–54.
Ma, K.T., Luo, Y., Kwan, T., Wu, Y., 2019. Mooring System Engineering for Offshore Structures. Gulf Professional Publishing.
Martinelli, L., Ruol, P., Cortellazzo, G., 2012. On mooring design of wave energy converters: the Seabreath application. Coast. Eng. Proc. 1 (3).
Pham, H.D., Cartraud, P., Schoefs, F., Soulard, T., Berhault, C., 2019. Dynamic modeling of nylon mooring lines for a floating wind turbine. Appl. Ocean Res. 87, 1–8.
SINTEF Ocean, 2017. RIFLEX 4.10.3 User Guide.
Silva, D., Bento, A.R., Martinho, P., Guedes Soares, C., 2015. High resolution local wave energy modelling for the Iberian Peninsula. Energy 91, 1099–1112.
Silva, D., Bento, A.R., Martinho, P., Guedes Soares, C., 2016. Corrigendum to "High resolution local wave energy modelling in the Iberian Peninsula. Energy 94, 857–858.
Silva, D., Martinho, P., Guedes Soares, C., 2018. Wave energy distribution along the Portuguese continental coast based on a thirty three years hindcast. Renew. Energy 127 (4), 1067–1075.
Thomsen, J.B., 2015. Mooring solutions for large wave energy converters. In: International Network on Offshore Renewable Energy (INORE): 11th International Symposium.
Thomsen, J.B., Ferri, F., Kofoed, J.P., 2016. Experimental testing of moorings for large floating wave energy converters. In: Guedes Soares, C. (Ed.), Progress in Renewable Energies Offshore. Taylor & Francis Group, London, UK, pp. 703–710.
Thomsen, J.B., Ferri, F., Kofoed, J.P., 2017a. Screening of available tools for dynamic mooring analysis of wave energy converters. Energies 10 (7), 853.
Thomsen, J.B., Kofoed, J.P., Ferri, F., Eskilsson, C., Bergdahl, L., Delaney, M., Thomas, S., Nielsen, K., Rasmussen, K.D., Friis-Madsen, E., 2017b. On mooring solutions for large wave energy converters. In: Proc Twelfth Eur Wave Tidal Energy Conf.
Thomsen, J.B., Ferri, F., Kofoed, J.P., Black, K., 2018. Cost optimization of mooring solutions for large floating wave energy converters. Energies 11 (1), 159.
Wang, S., Xu, S., Xiang, G., Guedes Soares, C., 2018. An overview of synthetic mooring cables in marine applications. In: Guedes Soares, C. (Ed.), Advances in Renewable Energies Offshore. Taylor & Francis Group, London, pp. 854–863.
Wang, S., Xu, S., Guedes Soares, C., Zhang, Y., Liu, H., Li, L., 2020. Experimental study of nonlinear behavior of a nylon mooring rope at different scales. In: Guedes Soares, C. (Ed.), Developments in Renewable Energies Offshore. Taylor and Francis, London, UK, pp. 690–697.
Waves4Power, 2018. WaveEL: demonstration site at Runde, Norway. https://www.waves4power.com/demo-runde/. (Accessed 14 February 2018).
Weller, S., Johanning, L., Davies, P., 2013. Best Practice Report–Mooring of Floating Marine Renewable Energy Devices. Deliverable 3.5.3 from the MERiFIC Project.
Weller, S.D., Johanning, L., Davies, P., Banfield, S.J., 2015. Synthetic mooring ropes for marine renewable energy applications. Renew. Energy 83, 1268–1278.
Weller, S.D., Hardwick, J., Gomez, S., Heath, J., Jensen, R., Mclean, N., Johanning, L., 2018. Verification of a rapid mooring and foundation design tool. Proc. Inst. Mech. Eng. Part M J Eng Marit Environ 232, 116–129.
Xiang, G., Xu, S., Wang, S., Guedes Soares, C., 2018. Comparative study on two different mooring systems for a buoy. In: Guedes Soares, C. (Ed.), Advances in Renewable Energies Offshore. Taylor & Francis Group, London, pp. 829–835.
Xu, S., Wang, S., Hallak, T.S., Rezanejad, K., Hinostroza, M.A., Guedes Soares, C., Rodriguez, C.A., Rosa-Santos, P., Taveira-Pinto, F., 2018a. Experimental study of two mooring systems for wave energy converters. In: Guedes Soares, C., Santos, T.A. (Eds.), Progress in Maritime Technology and Engineering. UK Taylor & Francis Group, London, pp. 667–676.
Xu, S., Ji, C., Guedes Soares, C., 2018b. Experimental study on taut and hybrid moorings damping and their relation with system dynamics. Ocean Eng. 154, 322–340.
Xu, S., Rezanejad, K., Gadelho, J.F.M., Wang, S., Guedes Soares, C., 2020b. Experimental investigation on a dual chamber floating oscillating water column moored by flexible mooring systems. Ocean Eng. 216, 108083.
Xu, S., Wang, S., Guedes Soares, C., 2019. Review of mooring design for floating wave energy converters. Renew. Sustain. Energy Rev. 111, 595–621.
Xu, S., Wang, S., Liu, H., Zhang, Y., Li, L., Guedes Soares, C., 2021a. Experimental evaluation of the dynamic stiffness of synthetic fibre mooring ropes. Appl. Ocean Res. 112, 102709.
Xu, S., Wang, S., Guedes Soares, C., 2020a. Experimental investigation on hybrid mooring systems for wave energy converters. Renew. Energy 158, 130–153.
Xu, S., Wang, S., Guedes Soares, C., 2021b. Experimental investigation on the influence of hybrid mooring system configuration and mooring material on the hydrodynamic performance of a point absorber. Ocean Eng. 233, 109178.
Xu, S., Wang, S., Guedes Soares, C., 2021c. Experimental study of the influence of the rope material on mooring fatigue damage and point absorber response. Ocean Eng. 232, 108667.
Yang, S.H., Ringsberg, J.W., Johnson, E., Hu, Z., Palm, J., 2016. A comparison of coupled and de-coupled simulation procedures for the fatigue analysis of wave energy converter mooring lines. Ocean Eng. 117, 332–345.
Yang, S.H., Ringsberg, J.W., Johnson, E., Hu, Z., Bergdahl, L., Duan, F., 2018. Experimental and numerical investigation of a taut-moored wave energy converter: a validation of simulated buoy motions. Proc. IME M J. Eng. Marit. Environ. 232 (1), 97–115.
Yang, S.H., Ringsberg, J.W., Johnson, E., Hu, Z., 2020. Experimental and numerical investigation of a taut-moored wave energy converter: a validation of simulated mooring line forces. Ships Offshore Struct. 15 (Suppl. 1), S55–S69.
Yang, S.H., Ringsberg, J.W., Johnson, E., Hu, Z., 2021. Experimental and numerical investigation of a taut-moored wave energy converter: a validation of simulated mooring line forces. Ships Offshore Struct. 15 (Suppl. 1), S55–S69.
Johanning, L., Smith, G.H. and Wolfram, J., 2005. Towards design standards for WEC moorings. In European Wave and Tidal Conference. EWTEC 2005, 29.08–02.09.2005, Glasgow, UK.